JOURNAL OF AGRICULTURAL AND FOOD CHEMISTRY

Almond (*Prunus dulcis* (Mill.) D.A. Webb) Skins as a Potential Source of Bioactive Polyphenols

MARIA MONAGAS,† IGNACIO GARRIDO,† ROSA LEBRÓN-AGUILAR,‡ BEGOÑA BARTOLOME,*,† AND CARMEN GÓMEZ-CORDOVÉS†

Instituto de Fermentaciones Industriales (CSIC), Juan de la Cierva 3, 28006 Madrid, Spain, and Instituto de Química-Física "Rocasolano" (CSIC), Serrano 119, 28006 Madrid, Spain

An exhaustive study of the phenolic composition of almond (*Prunus dulcis* (Mill.) D.A. Webb) skins was carried out in order to evaluate their potential application as a functional food ingredient. Using the HPLC-DAD/ESI-MS technique, a total of 33 compounds corresponding to flavanols, flavonols, dihydroflavonols and flavanones, and other nonflavonoid compounds were identified. Peaks corresponding to another 23 structure-related compounds were also detected. MALDI-TOF MS was applied to characterize almond skin proanthocyanidins, revealing the existence of a series of A- and B-type procyanidins and propelargonidins up to heptamers, and A- and B-type prodelphinidins up to hexamers. Flavanols and flavonol glycosides were the most abundant phenolic compounds in almond skins, representing up to 38–57% and 14–35% of the total quantified phenolics, respectively. Due to their antioxidant properties, measured as oxygen-radical absorbance capacity (ORAC) at 0.398–0.500 mmol Trolox/g, almond skins can be considered as a value-added byproduct for elaborating dietary antioxidant ingredients.

KEYWORDS: Almond skins; *Prunus dulcis*; polyphenols; procyanidins; propelargonidins; prodelphinidins; flavonols; flavanones; HPLC-DAD/ESI-MS; MALDI-TOF; antioxidants; ORAC

INTRODUCTION

Nuts are a food traditionally associated with the Mediterranean-type diet. Their regular consumption, in moderate doses, is related to a lower risk of cardiovascular diseases (*1–4*). The anticancer activity of nuts has also been demonstrated in experimental animals (*5*). These beneficial effects are mainly attributed to their lipid profile, arginine, fiber, and vitamin E contents as well as to other compounds with antioxidant properties, such as polyphenols (*6–12*).

Almonds (*Prunus dulcis* (Mill.) D.A. Webb) belong to the Rosaceae family and consist of an outer hull with an intermediate shell that contains a kernel or edible seed covered by a brown skin. The hull splits open when maturity is reached and is then separated from the shelled almond (whole natural almond). During some industrial processing of almonds, the skin (seed coat) is removed from the kernel by blanching and then discarded (*13*). For roasted almonds and other appetizers, skins are not removed. The skin, which has very low economic value, represents ∼4% of the total almond weight but contains 70–100% of total phenols present in the nut (*11*). Byproducts derived from almond industrial processing (skins, shells, and hulls) are normally used for livestock feed and as raw material for energy production. However, over the past few years, research has been conducted to evaluate the possible use of these byproducts as sources of compounds/fractions with antioxidant properties that could be used to control the oxidative process in the food industry or as functional ingredients for the elaboration of nutritional supplements (*6, 9, 10, 14–16*).

The phenolic composition of almond skins has not been extensively studied, probably due to its structural complexity, although both nonflavonoid and flavonoid compounds have been identified. Nonflavonoid compounds include protocatechuic, vanillic, and *p*-hydroxybenzoic acids (*6, 11*). Flavonoid compounds identified in the skin include compounds belonging to the group of flavanols, flavonols, dihydroflavonols, and flavanones. Very little data have been reported about proanthocyanidin composition of almond skins. Brieskorn and Betz (*17*) first identified the flavanol monomers (+)-catechin and (−)-epicatechin as well as dimers constituted by these units (procyanidins B1, B3, and B4) but not by trihydroxylated ones (i.e., gallocatechin and epigallocatechin). Lazarus et al. (*18*) confirmed the presence of B-type procyanidins, at the same time eliminating the presence of A-type procyanidins in almond skins. Later, Amarowicz et al. (*19*) reported the presence, in an almond seed crude extract, of procyanidins B2 and B3 as well as delphinidin and cyanidin after *n*-butanol–HCl hydrolysis. In the case of flavonols, the 3-*O*-glucosides, -galactosides, and -rutinosides of quercetin, kaempferol, and isorhamnetin, as well as their corresponding aglycones, have been identified in almond

* Corresponding author (Tel 34 91562900; Fax 34 915644853; e-mail bartolome@ifi.csic.es).
† Instituto de Fermentaciones Industriales.
‡ Instituto de Química-Física "Rocasolano".

10.1021/jf071780z CCC: $37.00
Published on Web 09/15/2007

skins (*6–9, 11*). Recently, morin (*9*) and dihydrokaempferol (*11*) were also found. Finally, the flavanones naringenin-7-*O*-glucoside, eriodictyol-7-*O*-glucoside, and eriodictyol-7-*O*-galactoside and their corresponding aglycones have been identified in almond skins (*6, 11*).

Around 12% of the world's almond production is grown in Spain. This leads to the accumulation of large amounts of byproducts and subsequent environmental problems due to their difficult degradation. On the other hand, natural antioxidants present in almond skins could contribute to the health benefits associated with almond consumption. The aim of the present work was to perform a thorough screening of the phenolic composition of almond skins with the aim of identifying new value-added antioxidant compounds that could permit this byproduct to be used as a raw material to produce dietary antioxidant ingredients.

MATERIALS AND METHODS

Commercial Standards and Reagents. (+)-Catechin, (−)-epicatechin, and disodium fluorescein were purchased from Sigma (St. Louis, MO); eriodictyol-7-*O*-glucoside, eriodictyol, quercetin-3-*O*-glucoside, quercetin, kaempferol-3-*O*-rutinoside, kaempferol-3-*O*-glucoside, dihydroquercetin, isorhamnetin-3-*O*-rutinoside, isorhamnetin-3-*O*-glucoside, isorhamnetin, naringenin-7-*O*-glucoside, naringenin, and kaempferol, from Extrasynthèse (Genay, France); chlorogenic acid, 6-hydroxy-2,5,7,8-tetramethylchroman-2-carboxylic acid (Trolox) and 2,2′-azobis(2-methylpropionamidine) dihydrochloride, from Aldrich (St. Louis, MO); protocatechuic aldehyde, *trans*-*p*-coumaric acid, *p*-hydroxybenzoic acid, vanillic acid, and protocatechuic acid, from Fluka (Buchs, Switzerland).

Extraction of Phenolic Compounds from Almond Skins. Almond skins corresponding to a mixture of Spanish varieties and to a mixture of American varieties (harvest 2004) were kindly supplied by La Morella Nuts (Tarragona, Spain). These two samples were mixtures representative of the almonds industrially processed in the geographical area of Tarragona (Spain). An industrial blanching process (95 °C, 3 min) was applied to remove the skins from the kernels. The skins were then oven-dried and milled in a Janke & Kunkel mill (Ika Labortechnik, Wilmington, NC). In a previous study (*20*), the mixture methanol/HCl (1000:1, v/v) was found the most effective one for antioxidant extraction from almond skins. The solid sample (2.10 g) was mixed with 30 mL of methanol/HCl (1000:1, v/v) and sonicated for 15 min followed by an extra 15 min resting period; this procedure was performed twice. The sample was then centrifuged (3024*g*, 10 min, 5 °C). The supernatant was separated, and the pellet was submitted to two further extractions. The supernatants were combined and the mixture was taken to dryness under vacuum. The residue was dissolved in 40 mL of distilled water and extracted with ethyl acetate (40 mL × 4). The organic phases were combined and dried with anhydrous Na_2SO_4 for 20 min. The extract was then taken to dryness under vacuum, dissolved in 2 mL of methanol/H_2O (50:50, v/v), and finally filtered (0.45 μm) for HPLC and MALDI-TOF analysis. The extractions were performed in duplicate.

Analysis of Phenolic Compounds by High Performance Liquid Chromatography (HPLC-DAD-Fluorescence and HPLC-DAD/ESI-MS). A Waters (Milford, MA) liquid chromatography system equipped with a 600-MS controller, a 717Plus autosampler, a 996 photodiode-array detector (DAD), and a fluorescence detector coupled to the Waters Empower (version 5.0) for data acquisition and processing was used. Separation was performed on a 250 × 4.6 mm r.d., 4 μm reversed-phase Nova-Pak C_{18} (Waters, Milford, MA) column at room temperature. A gradient consisting of solvent A (water/acetic acid, 98:2, v/v) and solvent B (water/acetonitrile/acetic acid, 73:25:2, v/v/v) was applied at a flow rate of 1.0 mL/min as follows (*21*): 0–80% B linear from 0 to 55 min, 80–90% B linear from 55 to 57 min, 90% B isocratic from 57 to 70 min, 90–95% B linear from 70 to 80 min, 95–100% B from 80 to 90 min, followed by washing (methanol) and reequilibration of the column from 90 to 120 min. A 75 μL volume sample was injected into the column. The detection conditions were 210–360 nm (DAD) and 280 and 310 nm for the emission and excitation filters, respectively (fluorescence detector). Quantification was carried out by external standard calibration curves. All of the phenolic compounds were quantified at 280 nm, except flavanols which were quantified by their fluorescence response. Because of the lack of commercial standards, oligomeric flavanols were quantified using the (−)-epicatechin calibration curve.

In addition to their UV spectra, the identification of phenolic compounds was also carried out by mass spectrometry coupled to HPLC. A Hewlett-Packard series 1100 (Palo Alto, CA) chromatography system equipped with a diode array detector (DAD) and a quadrupole mass spectrometer (Hewlett-Packard series 1100 MSD) with an electrospray interface was used. Separation conditions were the same as described above, except for the flow rate which was set to 0.7 mL/min. The ESI source parameters were as follows: drying gas (N_2) flow and temperature, 10 L/min and 350 °C, respectively; nebulizer pressure, 55 psi; capillary voltage, 4000 V. Mass spectra were obtained using in-source collision-induced dissociation mass spectrometry (CID MS), scanning negative ions from *m/z* 100 to *m/z* 2000 using the following fragmentation program: from *m/z* 0–200 (150 V) and from *m/z* 200–2000 (300 V).

MALDI-TOF Spectra. Samples (1 μL) were mixed with 4 μL of the matrix consisting of 2,5-dihydroxybenzoic acid (gentisic acid) at a concentration of 20 mg/mL in water. Then, 1 μL of this solution was spotted onto a flat stainless-steel sample plate and dried in air. MALDI-TOF measurements were performed using a Voyager DE-PRO mass spectrometer (Applied Biosystems, Foster City, CA) equipped with a pulsed nitrogen laser (λ = 337 nm, 10 ns pulse width, and 20 Hz frequency) and a delayed extraction ion source. Ions generated by the laser desorption were introduced into the flight tube (1.3 m flight path) with an acceleration voltage of 25 kV, 94% grid voltage, 0.05% ion guide wire voltage, and a delay time of 100 ns in the linear positive ion mode. All mass spectra were collected by averaging the signals of at least 3000 laser shots over the *m/z* range 300–6000. Angiotensin I and bovine insulin were used for external calibration.

Radical Scavenging Activity. To determine their antioxidant activity, ground skins (0.05 g) were extracted with 10 mL of methanol/HCl (1000:1, v/v) by sonication for 5 min followed by an extra 15 min resting period. The mixture was then centrifuged (3024*g*, 5 min, 5 °C) and filtered (0.45 μm). The radical scavenging activity of the extracts was determined by the ORAC method using fluorescein as a fluorescence probe (*22*). Briefly, the reaction was carried out at 37 °C in 75 mM phosphate buffer (pH 7.4), and the final assay mixture (200 μL) contained fluorescein (70 nM), 2,2′-azobis(2-methyl-propionamidine) dihydrochloride (12 mM), and antioxidant [Trolox (1–8 μM) or sample (at different concentrations)]. The plate was automatically shaken before the first reading, and the fluorescence was recorded every minute for 98 min. A Polarstar Galaxy plate reader (BMG Labtechnologies GmbH, Offenburg, Germany) with 485-P excitation and 520-P emission filters was used. The equipment was controlled by the Fluostar Galaxy software version (4.11-0) for fluorescence measurement. Black 96-well untreated microplates (Nunc, Denmark) were used. 2,2′-Azobis(2-methylpropionamidine) dihydrochloride and Trolox solutions were prepared daily and fluorescein was diluted from a stock solution (1.17 mM) in 75 mM phosphate buffer (pH 7.4).

All reaction mixtures were prepared in duplicate, and at least three independent runs were performed for each sample. Fluorescence measurements were normalized to the curve of the blank (no antioxidant). From the normalized curves, the area under the fluorescence decay curve (AUC) was calculated as

$$\mathrm{AUC} = 1 + \sum_{i=1}^{i=98} f_i/f_0$$

where f_0 is the initial fluorescence reading at 0 min and f_i is the fluorescence reading at time *i*. The net AUC corresponding to a sample was calculated as follows:

$$\mathrm{netAUC} = \mathrm{AUC}_{\mathrm{antioxidant}} - \mathrm{AUC}_{\mathrm{blank}}$$

The regression equation between net AUC and antioxidant concentration was calculated. The ORAC value was calculated by dividing the slope

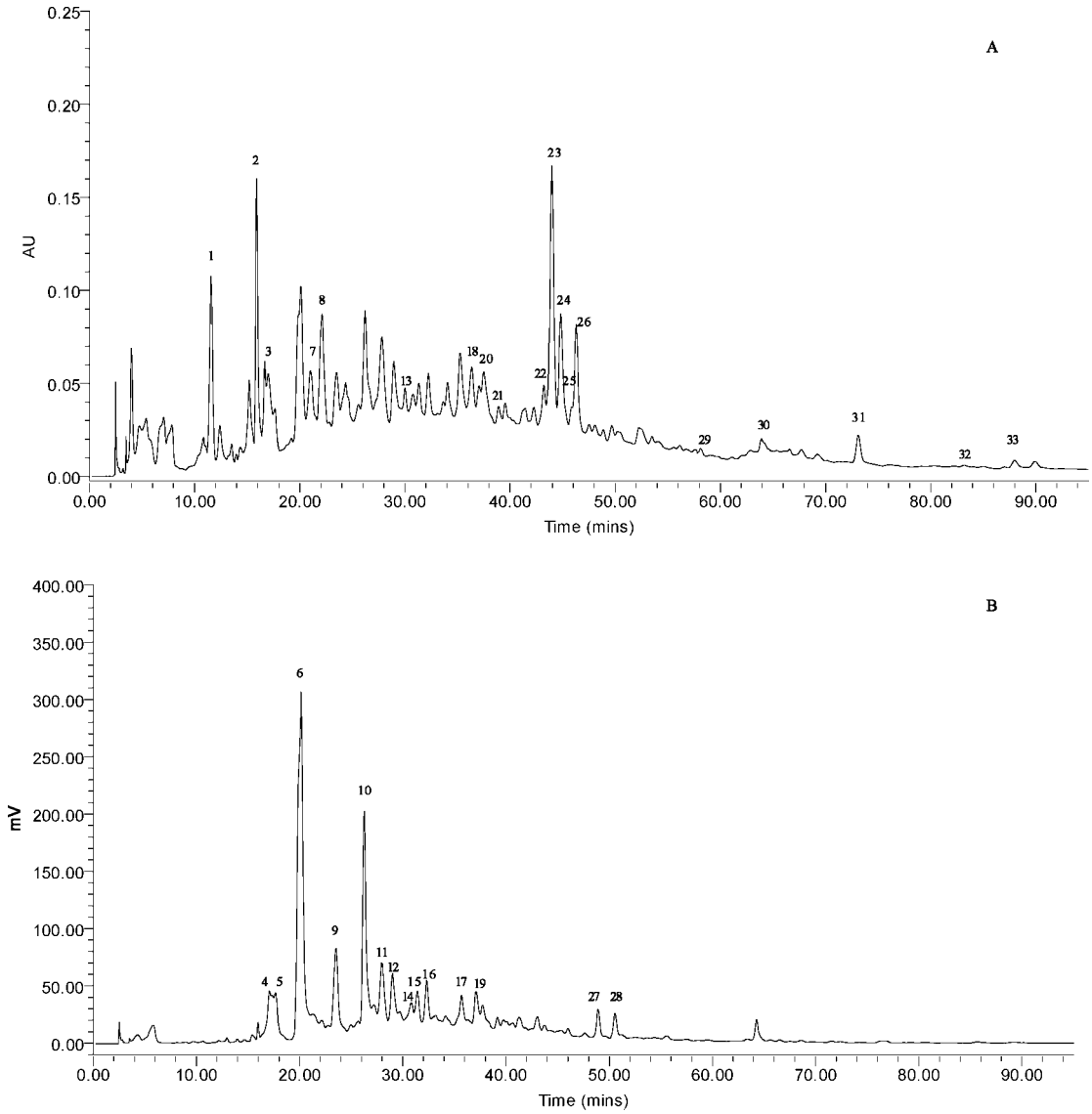

Figure 1. HPLC chromatograms of phenolic compounds in almond skins: (**A**) absorbance at 280 nm and (**B**) fluorescence. Peak numbers are referred to **Table 1**.

of the latter equation by the slope of the Trolox line obtained for the same assay. Final ORAC values were expressed as mmol of Trolox equiv/g of ingredient.

Statistical Analysis. ANOVA analysis was performed using the PC software package Statgraphics (versión 2.1; Statistical Graphics Corp. Rockville, MD).

RESULTS AND DISCUSSION

Identification of Phenolic Compounds in Almond Skins. **Figure 1** illustrates the HPLC chromatograms of the phenolic compounds from almond skins. Most phenolic compounds show absorbance at 280 nm (**Figure 1A**), although the fluorescence response ($\lambda_{excitation}$ = 280 nm, $\lambda_{emission}$ = 310 nm) is only characteristic of flavanols (**Figure 1B**). A total of 33 flavonoid (flavanols, flavonols, flavanonols or dihydroflavonols, and flavanones) and nonflavonoid compounds have been identified in almond skins on the basis of their retention time and UV and mass spectra (**Table 1**). In addition, 23 peaks corresponding to compounds with related structures have been detected (**Table 2**).

Flavanols. Flavanols or flavan-3-ols occurred as monomers, oligomers, and polymers, the latter also known as proanthocyanidins or condensed tannins. Monomeric units include afzelechin, catechin, and gallocatechin (2*R*:3*S* forms) and their diasteromers epiafzelechin, epicatechin, and epigallocatechin (2*S*:3*S* forms). Proanthocyanidins exclusively constituted by (epi)catechin are called procyanidins. Propelargonidins and prodelphinidins contain (epi)afzelechin and (epi)gallocatechin, respectively, and are usually mixed with procyanidins. With respect to the interflavanic bond nature, B-type procyanidins are those in which monomers are linked through the C-4 position of the top unit and the C-6 or C-8 positions of the terminal unit, the C4-C8 isomers being more abundant than the C4-C6 ones. A-type procyanidins also contain an ether-type bond between the C-2 position of the top unit and the hydroxyl group at C-5 or C-7 of the lower unit (*23*).

Peaks **6** and **10**, presenting a molecular ion ($[M–H]^-$) at *m*/*z* 289, corresponded to (+)-catechin and to (−)-epicatechin, respectively (**Figure 1**, **Table 1**). Peaks **4**, **5**, **9**, **12**, and **19** presented a $[M–H]^-$ at *m*/*z* 577, characteristic of B-type procyanidins: B3, B1, B2, B7, and B5, respectively (**Figure 1**, **Table 1**). The molecular ion at *m*/*z* 865, detected on peak **11**, corresponded to procyanidin C1, a B-type trimer (**Figure 1**, **Table 1**). The main mass fragments presented by dimeric and trimeric B-type procyanidins (**Figure 2A**,**C**) arose from the (a) retro-Diels–Alder (RDA) cleavage $[M–C_8H_8O_3–H]^-$ and sub-

Table 1. Phenolic Compounds Identified by HPLC-DAD/ESI(CID)-MS in Almond Skin Extracts

no.	compound	R_t (min)	λ_{max} (nm)	$[M-H]^-$ (*m*/*z*)	fragments (*m*/*z*)
1	protocatechuic acid	11.6	259.2, 293.5	153.0	109.1
2	protocatechuic aldehyde	15.9	280.4, 311.2	137.1	
3	*p*-hydroxybenzoic acid	17.0	255.2	137.1	
4	B3 [(+)-catechin-(4α→8)-(+)-catechin]	17.3	279.3	577.1	451.1, 425.1, 407.1, 289.1, 287.0
5	B1 [(−)-epicatechin-(4β→8)-(+)-catechin]	17.7	279.3	577.1	451.1, 425.1, 407.1, 289.1, 287.0
6	(+)-catechin	20.1	279.3	289.1	
7	chlorogenic acid	21.0	291.1, 319.5	353.0	
8	vanillic acid	22.1	262.7, 291.1	166.9	
9	B2 [(−)-epicatechin-(4β→8)-(−)-epicatechin]	23.5	279.3	577.1	451.1, 425.0, 407.0, 289.0, 287.0
10	(−)-epicatechin	26.3	279.3	289.0	
11	C1 [(−)-epicatechin-(4β→8)-(−)-epicatechin-(4β→8)-(−)-epicatechin]	27.8	279.3	865.2	739.2, 713.2, 695.0, 577.1, 575.1, 289.1, 287.0
12	B7 [(−)-epicatechin-(4β→6)-(+)-catechin]	28.9	279.3	577.2	451.0, 425.0, 406.9, 289.0, 287.0
13	*trans p*-coumaric acid	30.0	310.0	163.1	
14	trimer A [(epi)catechin-(epi)catechin→A→(epi)catechin]	30.8	279.3	863.1	710.9, 575.1
15	dimer A [(epi)catechin→A→(epi)catechin]	31.3	279.3	575.0	449.0, 289.0, 285.0
16	dimer A [(epi)catechin→A→(epi)catechin]	32.2	279.3	575.0	449.0, 289.1, 285.0
17	dimer A [(epi)catechin→A→(epi)catechin]	35.7	279.3	575.1	449.0, 289.0, 285.0
18	eriodictyol-7-*O*-glucoside	36.4	284.0	449.1	287.2
19	B5 [(−)-epicatechin-(4β→6)-(−)-epicatechin]	37.1	279.3	577.1	451.3, 425.1, 407.1, 289.1, 287.0
20	dihydroquercetin	37.5	288.3	303.0	
21	quercetin-3-*O*-glucoside	38.9	255.7, 354.0	463.1	301.0
22	kaempferol-3-*O*-rutinoside	43.2	265.1, 346.9	593.1	285.0
23	naringenin-7-*O*-glucoside	44.0	284.0	433.1	271.0
24	isorhamnetin-3-*O*-rutinoside	44.8	254.5, 355.2	623.1	315.0
25	kaempferol-3-*O*-glucoside	45.8	265.1, 346.9	447.0	285.0
26	isorhamnetin-3-*O*-glucoside	46.3	254.5, 354.0	477.1	315.0
27	dimer A [(epi)catechin→A→(epi)catechin]	48.9	279.3	575.0	449.0, 289.0, 285.0
28	dimer A [(epi)gallocatechin→A→(epi)catechin]	50.5	280.4	591.1	465.0, 301.1, 289.0
29	eriodictyol	58.1	287.5	287.0	
30	quercetin	63.9	255.2, 369.0	301.0	
31	naringenin	73.1	289.4	271.0	
32	kaempferol	83.2	265.1, 364.5	285.0	
33	isorhamnetin	88.0	254.5, 368.0	315.0	

Table 2. Mass-to-Charge Ratio (*m*/*z*) Signals Detected in Almond Skin Extracts

compound	R_t (min)	$[M-H]^-$ (*m*/*z*)	fragments (*m*/*z*)
benzoic alcohols and aldehydes			
eugenol	27.6	163.1	
p-hydroxybenzaldehyde	22.2	121.0	
procyanidins			
B-type trimers [(epi)catechin-(epi)catechin-(epi)catechin]	20.5, 26.6, 30.5	865.2	739.2, 713.2, 695.0, 577.2, 575.1, 289.0, 287.0
B-type tetramers [(epi)catechin-(epi)catechin-(epi)catechin-(epi)catechin]	20.0, 30.6	1153.3	865.2, 713.2, 577.2, 575.0, 289.0
A-type dimers [(epi)catechin→A→(epi)catechin]	46.1, 46.7	575.2	449.0, 289.0, 285.1
propelargonidins			
B-type dimers [(epi)afzelechin-(epi)catechin]	20.9, 28.1	561.3	435.0, 425.0, 407.0, 289.1, 271.0
B-type trimer [(epi)afzelechin-(epi)catechin-(epi)catechin]	31.5	849.2	577.0, 559.1, 289.0, 271.0
A-type dimer [(epi)afzelechin→A→(epi)catechin]	38.1	559.3	289.0
A-type trimer [(epi)catechin-(epi)catechin→A→(epi)afzelechin]	30.6	847.0	695.0, 559.0, 287.0
prodelphinidins			
A-type dimer [(epi)gallocatechin→A→(epi)catechin]	20.0	591.0	465.0, 289.0
glycosides and aglycones of flavonol and of dihydroflavonol			
dihydroquercetin-3-*O*-glucoside	20.3	465.0	303.0
dihydroquercetin-3-*O*-rutinoside	31.1	611.0	303.0
quercetin-3-*O*-galactoside	37.9	463.0	301.0
quercetin-3-*O*-rhamnoside	46.0	447.1	301.0
dihydrokaempferol	44.2	287.0	
dihydrokaempferol-3-*O*-glucoside	24.6	449.0	287.0
kaempferol-3-*O*-galactoside	45.2	447.0	285.0
isorhamnetin-3-*O*-galactoside	45.4	477.1	315.0

sequent elimination of a water molecule $[M–C_8H_8O_3–H_2O–H]^-$ (dimers: *m*/*z* 425, 407; trimers: *m*/*z* 713, 695), (b) interflavanic bond cleavage through the quinone–methine (QM) mechanism ($[M_{(top)}–3H]^-$ and $[M_{(bottom)}–H]^-$) (dimers: *m*/*z* 287, 289; trimers: *m*/*z* 287, 577 and 575, 289), and (c) heterocyclic ring fission (HRF) $[M–C_6H_6O_3–H]^-$ (dimers: *m*/*z* 451; trimers: *m*/*z* 739). Considering that the MS technique does not allow differentiation between the diasteromeric pairs (i.e., catechin vs epicatechin) nor elucidation of the position and stereochemistry of the interflavanic bond (C4–C8 vs C4–C6), the structural composition of the different B-type procyanidins was based on comparison with previously characterized procyanidin standards (*24*). In addition, peaks at *m*/*z* 865 corresponding to other three B-type procyanidin trimers (20.5, 26.6, and 30.5 min) as well as other peaks at *m*/*z* 1153 corresponding to two B-type tetramers (20.0 and 30.6 min) were also detected (**Table 2**, **Figure 2E**). As a

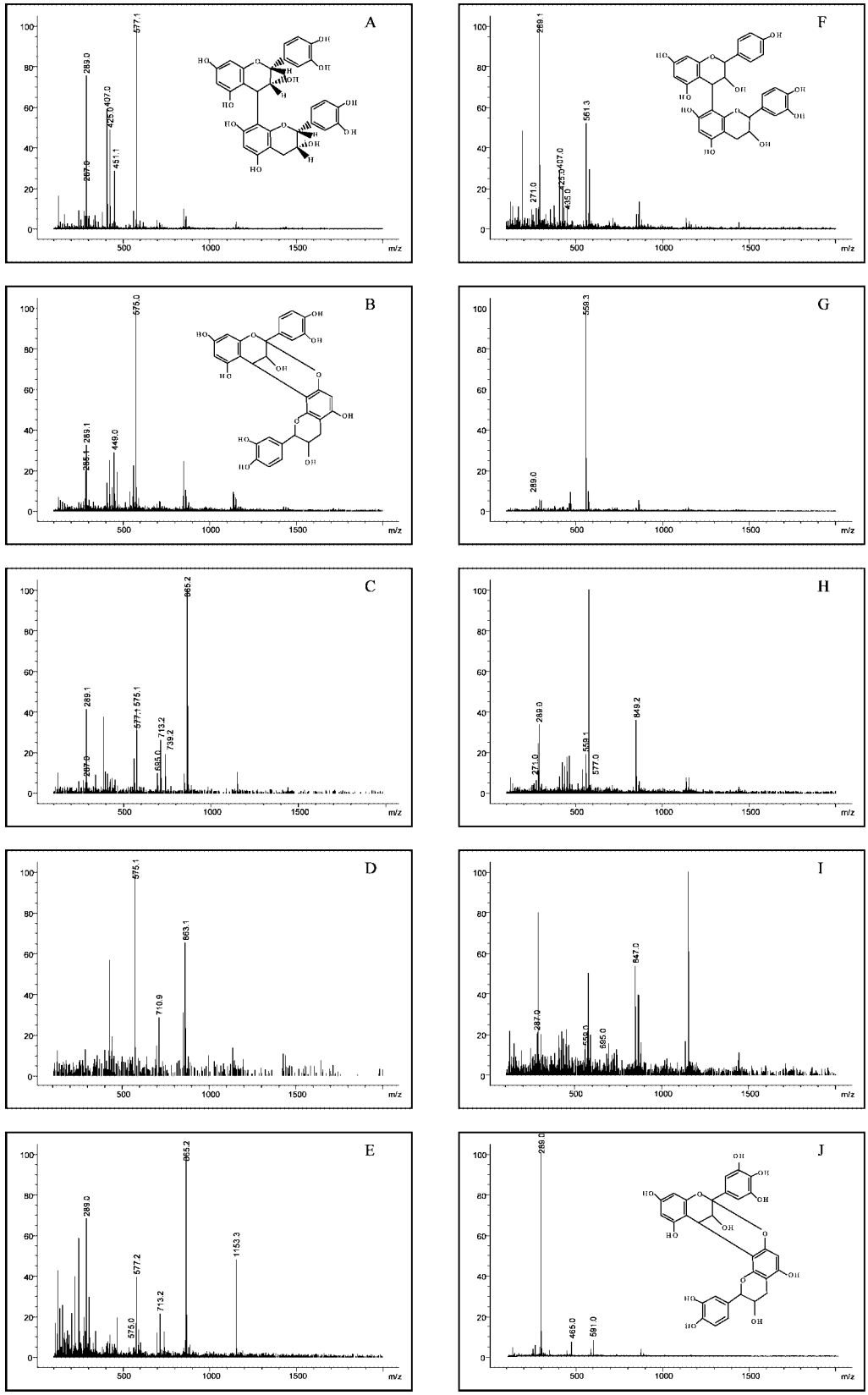

Figure 2. Negative-ion ESI(CID)-MS mass spectra of procyanidins **(A–E)**, propelargonidins **(F–I)**, and prodelphinidins **(J)** in almond skins: **(A)** dimer B2 [(−)-epicatechin-(4β→8)-(−)-epicatechin] (R_t = 23.5 min), **(B)** dimer A [(epi)catechin→A→(epi)catechin] (R_t = 31.3 min), **(C)** trimer C1 [(−)-epicatechin-(4β→8)-(−)-epicatechin-(4β→8)-(−)-epicatechin] (R_t = 27.8 min), **(D)** trimer A [(epi)catechin-(epi)catechin→A→(epi)catechin] (R_t = 30.8 min), **(E)** tetramer B [(epi)catechin-(epi)catechin-(epi)catechin-(epi)catechin] (R_t = 20.0 min), **(F)** dimer B [(epi)afzelechin-(epi)catechin] (R_t = 20.9 min), **(G)** dimer A [(epi)afzelechin→A→(epi)catechin] (R_t = 38.1 min), **(H)** trimer B [(epi)afzelechin-(epi)catechin-(epi)catechin] (R_t = 31.5 min), **(I)** trimer A [(epi)catechin-(epi)afzelechin→A→(epi)catechin] (R_t = 30.6 min), and **(J)** dimer A [(epi)gallocatechin→A→(epi)catechin] (R_t = 20.0 min).

result of the fragmentation of these tetrameric forms, a mass signal at *m*/*z* 865 was observed which was derived from the interflavanic bond cleavage between the first and second units, although the signal corresponding to its conjugate ion (*m*/*z* 287)

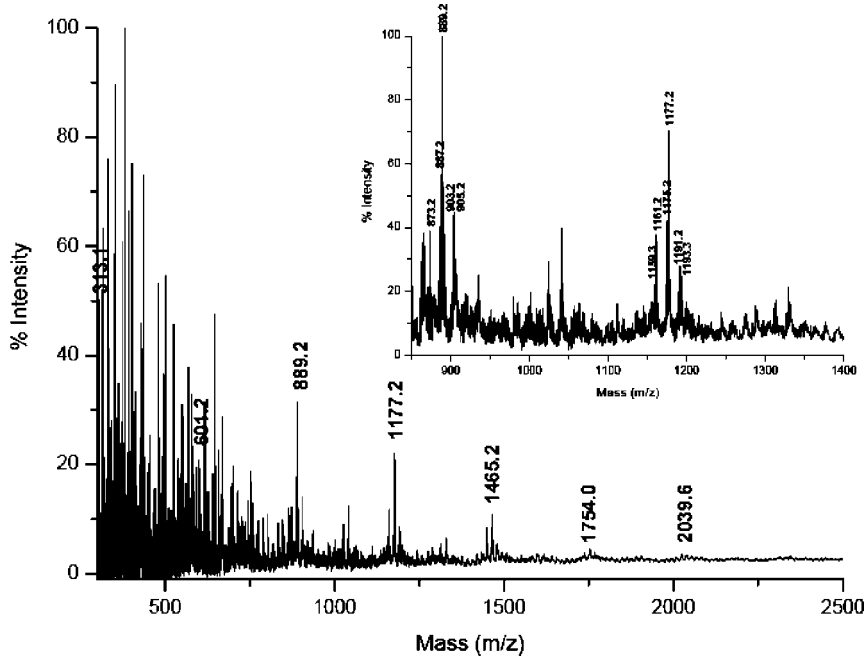

Figure 3. MALDI-TOF MS spectrum of almond skin extracts using 2,5-dihydroxybenzoic acid as matrix on linear positive ion mode.

was not detected. Other authors have also found a lower abundance of this fragment (quinone–methine) (*25*). The interflavanic bond cleavage could also occur between the second and third units (*m*/*z* 575 and 577) or between the third and fourth units (*m*/*z* 863 and 289). Finally, the signal at *m*/*z* 713 arose from RDA cleavage (−152 u) of the trimeric fragment (*m*/*z* 865).

Peaks **15**, **16**, **17**, and **27** showed a molecular ion (*m*/*z* 575) with 2 mass units lower than that of B-type dimers, suggesting an additional interflavanic bond which is characteristic of A-type procyanidins (**Table 1**, **Figure 2B**). The fragment at *m*/*z* 449 $[M–C_6H_6O_3–H]^-$ was generated from the heterocyclic ring fission of the top unit. The presence of the two A-type dimers with retention time at 46.1 and 46.7 min, respectively, was also confirmed by extraction of the ion at *m*/*z* 575 in the mass chromatograms (extracted ion chromatograms) (**Table 2**). Peak **14**, presenting a $[M–H]^-$ at *m*/*z* 863, corresponded to an A-type trimer (**Table 1**, **Figure 2D**). In this case, the fragment at *m*/*z* 575 arising from the interflavanic bond cleavage confirmed that the A-type linkage was located between the middle and bottom units [epi(catechin)-epi(catechin)→A→(epi)catechin], although its conjugated ion (*m*/*z* 287) could not be detected. Finally, the fragment at *m*/*z* 711 resulting from the RDA cleavage was also detected. Contrary to Lazarus et al. (*18*), who reported that almond skins only contained B-type procyanidins, our findings demonstrate for the first time the presence of A-type procyanidins in almond skins.

Peaks at *m*/*z* 561 (20.9 and 28.1 min) and at *m*/*z* 849 (31.5 min) (**Table 2**), both showing 16 mass units lower than B-type dimers and trimers, indicated the presence of an (epi)afzelechin unit instead of an (epi)catechin one, which is characteristic of propelargonidins. In both cases, ESI-MS fragmentation permitted elucidation of the position of the (epi)afzelechin unit in the oligomeric structure. In the case of dimers (*m*/*z* 561), the fragments at *m*/*z* 425 (−136 u) and at *m*/*z* 407 (−136-H_2O) arose from RDA cleavage and from the subsequent loss of a water molecule; the fragment at *m*/*z* 435 was from the heterocyclic ring fission, whereas those at *m*/*z* 271 and 289 were from the interflavanic bond cleavage (**Figure 2F**). The three type of cleavages indicated that the (epi)afzelechin unit was situated at the top position of the molecule. Considering the trimer (*m*/*z* 849), the fragments derived from the two possible interflavanic bond cleavages (*m*/*z* 559 and 289; 271 and 577) were detected, revealing that the (epi)afzelechin unit was also located at the top position of the molecule (**Figure 2H**). In addition, two other peaks (*m*/*z* 559 and 847) presenting 2 mass units lower than B-type dimeric and trimeric propelargonidins described above indicate the presence of an additional A-type bond within the structure (**Table 2**). In the case of the dimer (38.1 min) (*m*/*z* 559), the fragmentation was scarce, and only one signal at *m*/*z* 289 was detected (**Figure 2G**). In relation to the trimer (30.6 min) (*m*/*z* 847), the fragments at *m*/*z* 287 and 559, arising from the interflavanic bond cleavage between the top and middle units, indicated that the A-type linkage was situated between the middle and bottom units and that the (epi)afzelechin unit occupied the middle position. The fragment at *m*/*z* 695 was derived from the RDA cleavage of the top unit (**Figure 2I**). Although Gu et al. (*26*) have reported that (epi)afzelechin is a structural unit of almond proanthocyanidins, to our knowledge, this is the first time that A- and B-type propelargonidins have been identified in almond skins.

Besides propelargonidins, peak **28** showed a *m*/*z* of 591, 16 mass units more than A-type procyanidin dimers, which corresponded to an A-type prodelphinidin dimer (**Table 1**). A peak detected at *m*/*z* 591 (20.0 min) (**Figure 2J**) also corresponded to an A-type prodelphinidin dimer (**Table 2**). In both cases, the fragment at *m*/*z* 465 arose from the heterocyclic ring fission. For the compound **28**, the presence of fragments at *m*/*z* 301 and 289 suggested that the dimer contained (epi)gallocatechin as the top unit and (epi)catechin as the bottom unit [(epi)gallocatechin→A→(epi)catechin] (**Table 1**). For the signal at 20.0 min, the presence of fragment 289, which was also due to the coelution of (+)-catechin, together with the absence of a fragment at *m*/*z* 305 tentatively suggested that this dimer also contained (epi)gallocatechin as the top unit and (epi)catechin as the bottom unit (**Table 2**). This type of proanthocyanidin is also reported for the first time in almond skins.

Matrix-assisted laser desorption/ionization time-of-flight mass spectrometry (MALDI-TOF MS) was also applied to obtain additional information about the proanthocyanidin composition

Table 3. Proanthocyanidins Detected by MALDI-TOF-MS in Almond Skin Extracts

	structural unit			linkage		$[M + Na]^+$		
DP[a]	(epi)afzelechin	(epi)catechin	(epi)gallocatechin	A	B	calcd	obsd	PRO type[b]
1		1				313.3	313.1	
2	1	1		1		583.1	583.2	PEL
2	1	1			1	585.1	585.2	PEL
2		2		1		599.1	599.2	CYA
2		2			1	601.1	601.2	CYA
2		1	1	1		615.1	615.2	DEL
2		1	1		1	617.1	617.2	DEL
3	1	2			2	873.2	873.2	PEL
3		3		1	1	887.2	887.2	CYA
3		3			2	889.2	889.2	CYA
3		2	1	1	1	903.2	903.2	DEL
3		2	1		2	905.2	905.2	DEL
4	1	3		1	2	1159.2	1159.3	PEL
4	1	3			3	1161.3	1161.2	PEL
4		4		1	2	1175.2	1175.2	CYA
4		4			3	1177.3	1177.2	CYA
4		3	1	1	2	1191.2	1191.2	DEL
4		3	1		3	1193.2	1193.3	DEL
5	1	4			4	1449.3	1449.3	PEL
5		5		1	3	1463.3	1463.3	CYA
5		5			4	1465.3	1465.2	CYA
5		4	1	1	3	1479.3	1479.2	DEL
5		4	1		4	1482.3	1481.2	DEL
6	1	5			5	1737.4	1737.4	PEL
6		6		1	4	1751.4	1752.2	CYA
6		6			5	1753.4	1754.0	CYA
6		5	1	1	4	1767.3	1767.4	DEL
7	1	6		1	5	2023.4	2024.8	PEL
7	1	6			6	2025.4		PEL
7		7		1	5	2039.4	2039.6	CYA
7		7			6	2041.4		CYA

[a] *DP* = degree of polymerization. [b] PRO type = proanthocyanidin type; PEL = propelargonidin; CYA = procyanidin; DEL = prodelphinidin.

of almond skin extracts (**Figure 3**, **Table 3**). The MALDI-TOF spectrum provided masses (sodium adducts) corresponding to a series of A- and B-type oligomers and polymers composed either of pure (epi)catechin units (procyanidins) or mixed with (epi)afzelechin (propelargonidins) or (epi)gallocatechin (prodelphinidins) units. Procyanidins consisted of ions with the monoisotopic mass of 290.08 + 288.06 (*DP* – 1) − 2.02 (*A*) + 22.99 up to heptamers, where *DP* is the degree of polymerization and *A* is the number of A-type linkages. Using normal-phase HPLC-MS, Lazarus et al. (*18*) also reported a *DP* of 7 for single linked procyanidins in almond skin. Propelargonidins corresponded to the monoisotopic mass of 274.08 + 288.06 (*DP* – 1) − 2.02 (*A*) + 22.99 up to heptamers, which corresponded to structures containing only one (epi)afzelechin unit (**Table 3**). Finally, prodelphinidins were consistent with ions with a monoisotopic mass of 306.07 + 288.06 (*DP* – 1) − 2.02 (*A*) + 22.99 up to hexamers for structures containing only one (epi)gallocatechin unit (**Table 3**). Because of the low spectra resolution at high mass (heptamers), signals corresponding to A- and B-type procyanidin and propelargonidins overlapped (2024.8 and 2039.6, respectively) (**Table 3**). (Epi)catechins appeared to be the most abundant structural unit (**Figure 3**, **Table 3**), as occurs in other species (*24*). Considering the type of linkage, B-type linkages were more abundant than A-type ones. It is also important to highlight that, independently of DP, no more than one A-type linkage could be detected in the different structures (**Table 3**).

Very few foods were found to contain A-type proanthocyanidins. Apart for antioxidant and anti-inflammatory properties, these compounds have shown to prevent bacterial adhesion to the lining of the urinary tract -which reduces the risk of urinary tract infections- (*27*, *28*), and to improve glucose metabolism in type 2 diabetics (*29*).

Flavonols. The R_t, UV/vis spectra, and molecular ions of peaks **30**, **32**, and **33** matched those of the flavonols quercetin (*m*/*z* 301), kaempferol (*m*/*z* 285), and isorhamnetin (*m*/*z* 315) (**Figure 1**, **Table 1**). Peaks **21**, **25**, and **26** corresponded to the 3-*O*-glucoside derivatives of quercetin (*m*/*z* 463, 301), kaempferol (*m*/*z* 447, 285), and isorhamnetin (*m*/*z* 477, 315), whereas peaks **22** and **24** corresponded to the 3-*O*-rutinoside derivatives of kaempferol (*m*/*z* 593, 285) and isorhamnetin (*m*/*z* 623, 315), respectively (**Figure 1**, **Table 1**). Peaks were also detected at 37.9, 45.2, and 45.4 min, corresponding to the 3-*O*-galactoside derivatives of quercetin (*m*/*z* 463, 301), kaempferol (*m*/*z* 447, 285), and isorhamnetin (*m*/*z* 477, 315), respectively (**Table 2**). Finally, a signal at *m*/*z* 447, 301 (R_t = 46.0 min) was assigned to quercetin-3-*O*-rhamnoside (quercitrin), a compound detected for the first time in almond skins (**Table 2**).

Dihydroflavonols. Peak **20**, showing 2 mass units (*m*/*z* 303) more than quercetin, corresponded to dihydroquercetin (**Figure 1**, **Table 1**). In addition, peaks were also detected at 20.3 and 31.1 min, corresponding to dihydroquercetin-3-*O*-glucoside (*m*/*z* 465, 303) and to dihydroquercetin-3-*O*-rutinoside (*m*/*z* 611, 303) (**Table 2**). Dihydrokaempferol-3-*O*-glucoside and dihydrokaempferol were also detected at 24.6 min (*m*/*z* 449, 287) and at 44.2 min (*m*/*z* 287), respectively (**Table 2**). With the exception of the latter two compounds (*11*), the remaining dihydroflavanols have been identified in this work for the first time in almond skins.

Flavanones. Compounds identified as belonging to this family include naringenin (peak **31**, *m*/*z* 271) and its 7-*O*-glucoside derivative (peak **23**, *m*/*z* 433, 271), and peaks **29** and **18**, at *m*/*z* 287 and at *m*/*z* 449 and 287, which corresponded to eriodictyol and to eriodictyol-7-*O*-glucoside, respectively (**Figure 1**, **Table 1**).

Table 4. Content (μg/g) of Phenolic Compounds and ORAC Values (mmol of Trolox equiv/g) of Almond Skins[a]

	mixture of Spanish varieties	mixture of American varieties
hydroxybenzoic acids and aldehydes		
p-hydroxybenzoic acid	6.88 a	5.33 a
vanillic acid	14.5 b	7.65 a
protocatechuic acid	32.0 b	14.5 a
protocatechuic aldehyde	20.1 b	11.6 a
hydroxycinnamic acids		
trans-*p*-coumaric acid	traces	0.725
chlorogenic acid	10.6 b	3.12 a
procyanidins		
(+)-catechin	90.1 b	36.4 a
(−)-epicatechin	36.6 b	14.8 a
B3 + B1	23.8 b	11.8 a
B2	16.1 b	5.34 a
B7	13.9 b	5.63 a
B5	8.57 b	3.46 a
C1	15.3 b	3.45 a
A-type procyanidin dimer (tr = 31.3)	6.98 b	3.18 a
A-type procyanidin dimer (tr = 32.2)	6.30 b	1.36 a
A-type procyanidin dimer (tr = 35.7)	7.29 b	3.97 a
A-type procyanidin dimer (tr = 48.9)	2.04 b	0.70 a
A-type prodelphinidin dimer (tr = 50.7)	1.80 b	0.90 a
A-type procyanidin trimer (tr = 30.8)	4.28 b	1.58 a
flavonol glycosides		
kaempferol-3-*O*-rutinoside	12.8 a	31.8 b
kaempferol-3-*O*-glucoside	traces	1.65
isorhamnetin-3-*O*-rutinoside	27.6 a	41.4 b
isorhamnetin-3-*O*-glucoside	15.6 b	8.85 a
quercetin-3-*O*-glucoside	2.41 b	1.33 a
flavanone glycosides		
naringenin-7-*O*-glucoside	22.1 b	6.84 a
eriodictyol-7-*O*-glucoside	1.60 b	0.808 a
flavonol aglycones		
kaempferol	1.71	1.96
quercetin	1.78	1.43
isorhamnetin	4.87	4.19
dihydroflavonol aglycones		
dihydroquercetin	traces	traces
flavanone aglycones		
naringenin	2.83 a	4.01 b
eriodictyol	2.37 a	2.34 a
total of phenolic compounds	413 b	242 a
ORAC value	0.500 b	0.398 a

[a] Different letters in the same row indicate significant difference at $p < 0.05$.

Nonflavonoid Phenolic Compounds. Numerous hydroxybenzoic and hydroxycinnamic acids, alcohols, and benzoic aldehydes have been identified in almond skins. Peaks **1**, **3**, and **8**, corresponded to protocatechuic (*m*/*z* 153, 109), *p*-hydroxybenzoic (*m*/*z* 137), and vanillic (*m*/*z* 167) acids (**Figure 1**, **Table 1**). Peak **2**, exhibiting the same $[M–H]^-$ as *p*-hydroxybenzoic acid, corresponded to protocatechuic aldehyde. In addition, peaks at *m*/*z* 163 and at *m*/*z* 121 were also observed, corresponding to eugenol (27.6 min) and to *p*-hydroxybenzaldehyde (22.2 min), respectively (**Table 2**). The hydroxycinnamic acids identified include chlorogenic (3-caffeoylquinic) (peak **7**, *m*/*z* 353) and *trans*-*p*-coumaric (peak **13**, *m*/*z* 163) acids (**Figure 1**, **Table 1**). With the exception of hydroxybenzoic acids, the remaining compounds have been identified for the first time in almond skins.

Content of Phenolic Compounds in Almond Skins. Table 4 summarizes the content of phenolic compounds (μg/g) identified in almond skins. The total concentration of phenolic compounds was significantly higher in the almond skins from the mixture of Spanish varieties (413 μg/g) than in skins from the mixture of American varieties (242 μg/g). Flavanols (57% and 38% of the total phenolic content in skins from Spanish and American varieties, respectively) and flavonol glycosides (14% and 35%, respectively) were the most abundant phenolic compounds in the samples studied, followed by nonflavonoid-type phenolic compounds (20% and 18%, respectively). The remaining phenolic compounds (flavonol aglycones and flavanone glycosides and aglycones) represented 9% of total phenolic compounds quantified. In relation to flavanols, monomers represented 54–55% of the total flavanol quantified, followed by B-type (32–33%) and A-type (12–13%) procyanidins, although the individual concentrations of the latter ones were equal to or higher than some of the B-type procyanidins (i.e., B5). In relation to flavonol glycosides, rutinosides and in particular isorhamnetin-3-*O*-rutinoside (narcissin) were the most abundant forms.

Antioxidant Capacity of Almond Skin Extracts. The almond skin extracts were analyzed for their radical scavenging activity by the ORAC assay, a method previously used for studying the antioxidant activity of pure phenolic compounds (*22*) and other raw materials employed for the elaboration of antioxidant ingredients (*21*, *30*). The ORAC values were higher for the almond skins from the mixture of Spanish varieties (0.500 mmol Trolox/g) than for the skins from the mixture of American varieties (0.398 mmol Trolox/g), which is consistent with the contents of their compounds described above (**Table 3**). It is important to highlight that these ORAC values are in the range of values found for some byproducts derived from the winery industry, such as grape skins (0.428 mmol Trolox/g) (*25*) and seeds (2.11 mmol Trolox/g) (*21*), using the same solvent solutions and extraction procedure. This comparison suggests that almond skins could be considered as a

value-added byproduct to be used in the elaboration of antioxidant dietary ingredients.

The positive health effects associated with the consumption of almonds could be partly due to the almond skin phenolic composition, as this paper shows that almond skins comprise diverse well-known bioactive polyphenols, in particular flavanols and flavonols. In fact, the bioavailability (absorption, distribution, metabolism, and elimination) of these compounds, given individually or combined, as a standard or as a food component, has been demonstrated in numerous studies. Flavanol monomers, such as (+)-catechin and (−)-epicatechin, are absorbed faster than flavonols (*4*, *31*, *32*). In addition, the chemical structure of flavonols substantially influences the pharmacokinetics of these compounds. Derivatives containing rhamnose, such as rutinosides, which are largely present in almond skins, are absorbed ~10 times less than quercetin-4′-glucoside. Owing to their minimal absorption in the small intestine, these compounds are transferred to the large intestine where they are degraded by the rhamnosidases of the intestinal microbiota (*33*). The microbiota also plays an important role in the case of oligomeric and polymeric flavanols (proanthocyanidins), which are not absorbed in the small intestine either (*34*). Considering the occurrence of both rutinosides of flavonol and proanthocyanidins in almond skins, future research will be based on studying phenolic metabolites derived from the intestinal microbiota in order to evaluate the bioavailability of the almond skin phenols and its potential use as an antioxidant dietary ingredient.

LITERATURE CITED

(1) Jenkins, D. J.; Kendall, C. W.; Marchie, A.; Parker, T. L.; Connelly, P. W.; Qian, W.; Haight, J. S.; Faulkner, D.; Vidgen, E.; Lapsley, K. G.; Spiller, G. A. Dose response of almonds on coronary heart disease risk factors: blood lipids, oxidized low density-liproteins, lipoprotein(a), homocysteine, and pulmonary nitric oxide: a randomized, controlled, crossover trial. *Circulation* **2002**, *106*, 1327–1332.

(2) Milbury, P.; Chen, C. Y.; Kwak, H. K; Blumberg, J. Almond skins polyphenolics act synergistically with α-tocopherol to increase the resistance of low-density lipoproteins to oxidation. *Free Radical Res.* **2002**, *36*, 78–80.

(3) Salas-Salvadó, J.; García-Lorda, P.; Ros, E. Fibra, frutos secos y enfermedades cardivasculares. In *Frutos secos, salud y culturas mediterraneas*; Salas-Salvadó, J., Ros, E., Sabaté, J., Eds.; Editorial Glosa: Barcelona, 2005; p 157.

(4) Chen, C. Y.; Milbury, P. E.; Lapsley, K.; Blumberg, J. B. Flavonoids from almond skins are bioavailable and act synergistically with vitamins C and E to enhance hamster and human LDL resistance to oxidation. *J. Nutr.* **2005**, *135*, 1366–1373.

(5) Davis, P. A.; Iwashashi, C. K. Whole almonds and almond fractions reduce aberrant crypt foci in a rat model of colon carcinogenesis. *Cancer Lett.* **2001**, *165*, 27–33.

(6) Sang, S.; Lapsley, K.; Jeong, W.-S.; Lachance, P. A.; Ho, C.-T.; Rosen, R. T. Antioxidant phenolic compounds isolated from almond skins (Prunus amygdalus Batsch). *J. Agric. Food Chem.* **2002**, *50*, 2459–2463.

(7) Frison, S.; Sporns, P. Identification and quantification of flavonol glycosides in almond seedcoats using MALDI-TOF MS. *J. Agric. Food Chem.* **2002**, *50*, 2782–2787.

(8) Frison, S.; Sporns, P. Variation in the flavonol glycoside composition of almond seedcoats as determined by MALDI-TOF mass spectrometry. *J. Agric. Food Chem.* **2002**, *50*, 6818–6822.

(9) Wijeratne, S. S. K.; Abou-Zaid, M. M.; Shahidi, F. Antioxidant polyphenols in almond and its coproducts. *J. Agric. Food Chem.* **2006**, *54*, 312–318.

(10) Wijeratne, S. S. K.; Amarowicz, R.; Shahidi, F. Antioxidant activity of almonds and their by-products in food model systems. *J. Am. Oil. Chem. Soc.* **2006**, *83*, 223–230.

(11) Milbury, P. E.; Chen, C. Y.; Dolnikowski, G. G.; Blumberg, J. B. Determination of flavonoids and phenolics and their distribution in almonds. *J. Agric. Food Chem.* **2006**, *54*, 5027–5033.

(12) Chen, C. Y.; Lapsley, K.; Blumberg, J. B. A nutrition and health perspective on almonds. *J. Sci. Food Agric.* **2006**, *86*, 2245–2250.

(13) Vargas F. J. Árboles productores de frutos secos. Origen, descripción, distribución y producción. In *Frutos secos, salud y culturas mediterraneas*; Salas-Salvadó, J., Ros, E., Sabaté, J., Eds.; Editorial Glosa: Barcelona, 2005; p 21.

(14) Siriwardhana, S. S. K. W.; Shahidi, F. Antiradical activity of extracts of almond and its by-products. *J. Am. Oil. Chem. Soc.* **2002**, *79*, 903–908.

(15) Takeoka, G. R.; Dao, L. T. Antioxidant constituents of almond [Prunus dulcis (Mill.) D. A. Webb] hulls. *J. Agric. Food Chem.* **2003**, *51*, 496–501.

(16) Pinelo, M.; Rubilar, M.; Sineiro, J.; Núñez, M. J. Extraction of antioxidant phenolics from almond hulls (Prunus amygdalus) and pine sawdust (Pinus pinaster). *Food Chem.* **2004**, *85*, 267–273.

(17) Brieskon, C. H.; Betz, R. Procyanidin polymers crucial to the structure of the almond seed coat. *Z. Lebensm-Unters-Forsch.* **1998**, *187*, 347–353.

(18) Lazarus, S. A.; Adamson, G. E.; Hammerstone, J. F.; Schmitz, H. H. High performance liquid chromatography/mass spectrometry analysis of proanthocyanidins in food and beverages. *J. Agric. Food Chem.* **1999**, *47*, 3693–3701.

(19) Amarowicz, R.; Troszynska, A.; Shahidi, F. Antioxidant activity of almond seed extract and its fractions. *J. Food Lipids.* **2005**, *12*, 344–358.

(20) Garrido, I.; Monagas, M.; Gómez-Cordovés, C.; Bartolomé, B. Extraction of antioxidants from almond-processing by-products. *Grasas Aceites* **2007**, *58*, 130–135.

(21) Monagas, M.; Hernández-Ledesma, B.; Garrido, I.; Martín-Alvarez, P. J.; Gómez-Cordovés, C.; Bartolomé, B. Quality assessment of commercial dietary antioxidant products fromVitis vinifera L. grape seeds. *Nutr. Cancer* **2005**, *53*, 244–254.

(22) Dávalos, A.; Gómez-Cordovés, C.; Bartolomé, B. Extending applicability of the oxygen radical absorbance capacity (ORAC-fluorescein) assay. *J. Agric. Food Chem.* **2004**, *52*, 48–54.

(23) Porter, L. J. Flavans and proanthocyanidins. In *The Flavonoids*, Harbone, J. B., Ed.; Champam and Hall: New York, 1988; p 21.

(24) Monagas, M.; Gómez-Cordovés, C.; Bartolomé, B.; Laureano, O.; Ricardo da Silva, J. M. Monomeric, oligomeric and polymeric flavan-3-ol composition of wines and grapes from Vitis vinifera L. cv. Graciano, Tempranillo and Cabernet Sauvignon. *J. Agric. Food Chem.* **2003**, *51*, 6475–6481.

(25) Friedrich, W.; Eberhardt, A.; Galesa, R. Investigation of proanthocyanidins by HPLC with electrospray ionization mass spectrometry. *Eur. Food Res. Technol.* **2000**, *211*, 54–64.

(26) Gu, L.; Kelm, M. A.; Hammerstone, J. F.; Beecher, G.; Holden, J.; Haytowitz, D.; Prior, R. L. Screening of foods containing proanthocyanidins and their structural characterization using LC-MS/MS and thiolytic degradation. *J. Agric. Food Chem.* **2003**, *51*, 7513–7521.

(27) Foo, L. Y.; Lu, Y. R.; Howell, A. B.; Vorsa, N. A-type proanthocyanidin trimers from cranberry that inhibit adherence of uropathogenic P-fimbriated Escherichia coli. *J. Nat. Prod.* **2000**, *63*, 1225–1228.

(28) Foo, L. Y.; Lu, Y. R.; Howell, A. B.; Vorsa, N. The structure of cranberry proanthocyanidins which inhibit adherence of uropathogenic P-fimbriated Escherichia coli in vitro. *Phytochemistry* **2000**, *54*, 173–181.

(29) Anderson, R. A.; Broadhurst, C. L.; Polansky, M. M.; Schmidt, W. F.; Khan, A.; Flanagan, V. P.; Shoene, N. W.; Graves, D. J. Isolation and characterization of polyphenol type-A polymers from cinnamon with insulin-like biological activity. *J. Agric. Food Chem.* **2004**, *52*, 65–70.

(30) Monagas, M.; Hernández-Ledesma, B.; Gómez-Cordovés, C.; Bartolomé, B. Commercial dietary ingredients from Vitis vinifera L. leaves and grape skins: antioxidant and chemical characterization. *J. Agric. Food Chem.* **2006**, *54*, 319–327.

(31) Manach, C.; Texier, O.; Morand, C.; Crespy, V.; Regerat, F.; Demingné, C.; Rémésy, C. Comparison of the bioavailability of quercetin and catechin in rats. *Free Radical Biol. Med.* **1999**, *27*, 1259–1266.

(32) Baba, S.; Osakabe, N.; Natsume, M.; Muto, Y.; Takizawa, T.; Terao, J. In vivo comparison of the bioavailability of (+)-catechin, (-)-epicatechin and their mixtures in orally administered rats. *J. Nutr.* **2001**, *131*, 2885–2891.

(33) Manach, C.; Morand, C.; Demingné, C.; Texier, O.; Regerat, F.; Rémésy, C. Bioavailability of rutin and quercetin in rats. *FEBS Lett.* **1997**, *409*, 2–16.

(34) Manach, C.; Scalbert, A.; Morand, C.; Rémésy, C.; Jiménez, L. Polyphenols: food sources and bioavailability. *Am. J. Clin. Nutr.* **2004**, *79*, 727–47.

Received for review June 16, 2007. Revised manuscript received July 24, 2007. Accepted July 25, 2007. This work received financial support from Projects AGL2003-01088 and AGL2004-07075-C02-02. I.G. was the recipient of a fellowship from the I3P Program funding by the European Social Fund.

JF071780Z